



TOXICOLOGICAL REVIEW

OF

TRICHLOROETHYLENE

APPENDIX F

(CAS No. 79-01-6)

**In Support of Summary Information on the
Integrated Risk Information System (IRIS)**

September 2011

F. NONCANCER DOSE-RESPONSE ANALYSES

F.1. DATA SOURCES

Data sources are cited in the body of this report in the section describing dose-response analyses (see Chapter 5).

F.2. DOSIMETRY

This section describes some of the more detailed dosimetry calculations and adjustments used in Section 5.1.

F.2.1. Estimates of TCE in Air From Urinary Metabolite Data Using Ikeda et al. (1972)

F.2.1.1. Results for Chia et al. (1996)

Chia et al. (1996) demonstrated a dose-related effect on hyperzoospermia in male workers exposed to TCE, lumping subjects into four groups based on range of TCA in urine (see Table F-1).

Table F-1. Dose-response data from Chia et al. (1996)

TCA, mg per g creatinine ^a	Number of subjects	Number with hyperzoospermia
0.8–<25	37	6
50–<75	18	8
75–<100	8	4
≥100–136.4	5	3

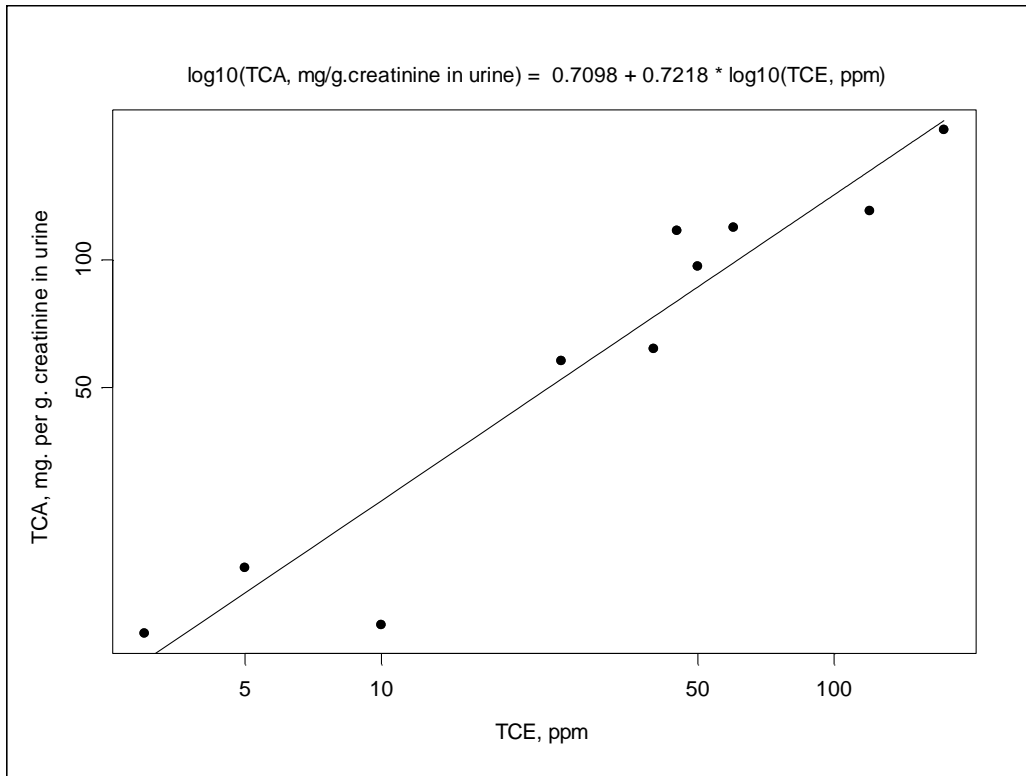
^aMinimum and maximum TCA levels are reported in the text of Chia et al. (1996), the other data, in their Table 5.

Data from Ikeda et al. (1972) were used to estimate the TCE exposure concentrations corresponding to the urinary TCA levels reported by Chia et al. (1996). Ikeda et al. (1972) studied 10 workshops, in each of which TCE vapor concentration was “relatively constant.” They measured atmospheric concentrations of TCE and concentrations in workers’ urine of TTCs, TCA, and creatinine, and demonstrated a linear relation between TTC/creatinine (mg/g) in urine and TCE in the work atmosphere. Their data are tabulated as geometric means (the last column was calculated by U.S. EPA, as described in Table F-2).

Table F-2. Data on TCE in air (ppm) and urinary metabolite concentrations in workers reported by Ikeda et al. (1972)

n	TCE (ppm)	TTC (mg/L)	TCA (mg/L)	TTC (mg/g creatinine)	TCA (mg/g creatinine)
9	3	39.4	12.7	40.8	13.15127
5	5	45.6	20.2	42.4	18.78246
6	10	60.5	17.6	47.3	13.76
4	25	164.3	77.2	122.9	57.74729
4	40	324.9	90.6	221.2	61.68273
5	45	399	138.4	337.7	117.137
5	50	418.9	146.6	275.8	96.52012
5	60	468	155.4	359	119.2064
4	120	915.3	230.1	518.9	130.4478
4	175	1,210.9	235.8	1,040.1	202.5399

These data were used to construct the last column as follows: $TCA (mg/g \text{ creatinine}) = TCA (mg/L) \times TTC (mg/g \text{ creatinine}) / TTC (mg/L)$. The regression relation between TCE (ppm) and TCA (mg/g creatinine) was evaluated using these data. Ikeda et al. (1972) reported that the measured values are lognormally distributed and exhibit heterogeneity of variance, and that the reported data (above) are geometric means. Thus, the regression relation between $\log_{10}(TCA [mg/g \text{ creatinine}])$ and $\log_{10}(TCE [ppm])$ was used, assuming constant variances and using number of subjects “*n*” as weights. Figure F-1 shows the results.



Coefficients:

	Value	Std. Error	t value	Pr(> t)
(Intercept)	0.7098	0.1132	6.2688	0.0002
log10(TCE.ppm)	0.7218	0.0771	9.3578	0.0000

Residual standard error: 0.3206 on 8 degrees of freedom
Multiple R-Squared: 0.9163
F-statistic: 87.57 on 1 and 8 degrees of freedom, the p-value is 0.0000139

Figure F-1. Regression of TCE in air (ppm) and TCA in urine (mg/g creatinine) based on data from Ikeda et al. (1972).

Next, a Berkson setting for linear calibration was assumed, in which one wants to predict X (TCE, ppm) from means for Y (TCA, mg/g creatinine), with substantial error in Y (Snedcor and Cochran, 1980). Thus, the inverse prediction for the data of Chia et al. (1996) was used to infer their mean TCE exposures. The relation based on data from Ikeda et al. (1972) is:

$$\log_{10}(\text{TCA, mg/g creatinine}) = 0.7098 + 0.7218 \times \log_{10}(\text{TCE, ppm}) \quad (\text{Eq. F-1})$$

and the inverse prediction is

$$\begin{aligned} \log_{10}(\text{TCE}) &= [\log_{10}(\text{TCA}) - 0.7098]/0.7218 \\ \text{TCE, ppm} &= 10^{([\log_{10}(\text{TCA}) - 0.7098]/0.7218)} \end{aligned} \quad (\text{Eq. F-2})$$

Because of the lognormality of data reported by Ikeda et al. (1972), the means of the logarithms of the ranges for TCA (mg/g creatinine) in Chia et al. (1996), which are estimates of the median for the group, were used. The results are shown in Table F-3.

Table F-3. Estimated urinary metabolite and TCE air concentrations in dose groups from Chia et al. (1996)

TCA, mg per g Creatinine	Estimated TCA median ^a	Log10(TCA median)	Estimated ppm TCE ^b
0.8–<25	4.47	0.650515	0.827685
50–<75	61.2	1.787016	31.074370
75–<100	86.6	1.937531	50.226119
≥100–136.4	117	2.067407	76.008668

^a10^{^(mean[log10(TCA limits in first column)])}.

^b10^{^([log10(TCA median)] – 0.7098)/0.7218}.

Dose-response relations for the data of Chia et al. (1996) were modeled using both the estimated medians for TCA (mg/g creatinine) in urine and estimated TCE (ppm in air) as doses. The TCE-TCA-TTC relations are linear up to about 75 ppm TCE (Figure 1 of Ikeda et al. (1972)), and certainly in the range of the BMD. As noted (see Section F.2.2), the occupational exposure levels are further adjusted to equivalent continuous exposure for deriving the POD.

F.2.1.2. Results for Mhiri et al. (2004)

The LOAEL group for abnormal trigeminal nerve somatosensory evoked potential reported in Mhiri et al. (2004) had a urinary TCA concentration of 32.6 mg TCA/mg creatinine. Using Eq. F-2, above gives an occupational exposure level = 10^{^([log10(32.6) – 0.7098]/0.7218)} = 12.97404 ppm. As noted below (see Section F.2.2), the occupational exposure levels are further adjusted to equivalent continuous exposure for deriving the POD.

F.2.2. Dose Adjustments to Applied Doses for Intermittent Exposure

The nominal applied dose was adjusted for exposure discontinuity (e.g., exposure for 5 days/week and 6 hours/day reduced the dose by the factor [5/7] × [6/24]). The PBPK dose-metrics took into account the daily and weekly discontinuity to produce an equivalent average dose for continuous exposure. No dose adjustments were made for duration of exposure or a less-than-lifetime study, as is typically done for cancer risk estimates, though in deriving the

candidate reference values, an UF for subchronic-to-chronic exposure was applied where appropriate.

For human occupational studies, inhalation exposures (air concentrations) were adjusted by the number of work (vs. nonwork) days and the amount of air intake during working hours as a fraction of the entire day (10 m^3 during work/ 20 m^3 for entire day). For the TCE ppm in air converted from urinary metabolite data using Ikeda et al. (1972), the work week was 6 days, so the adjustment for number of work days is 6/7.

F.2.3. Estimation of the Applied Doses for the Oral Exposures via Drinking Water and Feed

When oral doses were not reported in mg/kg/day and when study-specific data were not available for body weight and/or consumption rate, standard generic sex/strain-specific values from U.S. EPA (1988) were used to convert doses (e.g., in ppm in water) to doses in mg/kg/day.

For the feed study of George et al. (1986), study-specific data were used to estimate the applied dose. Female F334 rats were exposed for 19 weeks in their feed. Average body weights (W_t) are reported (Table A2, p. 53) for time periods having durations (d_t) of 1–4 weeks. Proportions of the 19 weeks of feeding were calculated for each time period as

Average daily feed consumed (F_t) is reported (Table A3) for the same time periods as body weight. Concentration (%w/w) of TCE in feed (Table 1, p.31) is reported for weeks 1, 6, 12, and 18.¹³ Two determinations are reported, which we averaged. The grouping of TCE feed concentrations into time periods (Table 1) differs from that used for body weight and feed consumption (Tables A2, A3). This was reconciled by linear interpolation of feed concentrations to produce concentrations (denoted C_t) for the time periods presented in Tables A2 and A3. We then calculated mg TCE consumed per kg-day, for each time period, as the product of:

$C_t/100$	feed concentration, %w/w, divided by 100 to give a fraction
F_t	feed consumed (grams)
1,000	1,000 (conversion of grams to mg)
$1/W_t$	1/[body weight, kg]

And found the TWA of these for each dose group:

¹³“Study Week 1” is repeated in the table, which is a typo for week 6, confirmed positively by the text on pages 19–20: “Analysis of Task 2 feed formulations at six week intervals ... Similarly, during week 6 of Task 2, the 0.15%, 0.30%, and 0.60% TCE formulations assayed at 27%, 71% and 82% of the theoretical concentration, respectively (Table 1)”.

The results were:

Nominal %w/w concentration in feed	Calculated mg/kg/day
0	0
0.15	72
0.30	186
0.60	389

F.2.4. PBPK Model-Based Internal Dose-Metrics

PBPK modeling was used to estimate levels of dose-metrics corresponding to different exposure scenarios in rodents and humans (see Section 3.5). The selection of dose-metrics for specific organs and endpoints is discussed under Section 5.1.

The PBPK model requires an average body weight. For most of the studies, averages specific to each species, strain, and sex were used. Where these were not reported in the text of an article, data were obtained by digitizing the body weight graphics ([Maltoni et al., 1986](#)) or by finding the median of weekly averages from graphs ([NTP, 1990, 1988](#); [NCL, 1976](#)). Where necessary, default adult body weights specific to the strain were used ([U.S. EPA, 1988](#)).

F.3. DOSE-RESPONSE MODELING PROCEDURES

Where adequate dose-response data were available, models were fitted with the BMDS (<http://www.epa.gov/ncea/bmds>) using the applicable applied doses or PBPK model-based dose-metrics for each combination of study, species, strain, sex, endpoints, and BMR under consideration.

F.3.1. Models for Dichotomous Response Data

F.3.1.1. Quantal Models

For dichotomous responses, the log-logistic, multistage, and Weibull models were fitted. These models adequately describe the dose-response relationship for the great majority of data sets, specifically in past TCE studies ([Filipsson and Victorin, 2003](#)). If the slope parameter of the log-logistic model was <1 , indicating a supralinear dose-response shape, then the model with the slope constrained to 1 was also fitted for comparison. For the multistage model, an order one less than the number of dose groups was used, in addition to the 2nd-order multistage model if it differed from the preceding model, and the first-order ('linear') multistage model (which is

identical to a Weibull model with power parameter equal to 1). The Weibull model with the power parameter unconstrained was also fitted t.

F.3.1.2. Nested Dichotomous Models

In addition, nested dichotomous models were used for developmental effects in rodent studies to account for possible litter effects, such as maternal covariates or intralitter correlation. The available nested models in BMDS are the nested log-logistic model, the Rai-VanRyzin models, and the NCTR model. Candidates for litter-specific covariates (LSC) were identified from the studies and considered legitimate for analysis if they were not significantly dose-related (determined via regression, ANOVA). The need for a LSC was indicated by a difference of at least 3 in the AIC for models with and without a LSC. The need to estimate intralitter correlations (IC) was determined by presence of a high correlation coefficient for at least one dose group and by AIC. The fits for nested models were also compared with the results from quantal models.

F.3.2. Models for Continuous Response Data

For continuous responses, the distinct models available in BMDS were fitted: power model (power parameter unconstrained and constrained to ≥ 1), polynomial model, and Hill model. Both constant variance and modeled variance models were fit; but constant variance models were used for model parsimony unless the p -value for the test of homogenous variance was < 0.10 , in which case the modeled variance models were considered. For the polynomial model, model order was selected as follows. A model of order 1 was fitted first. The next higher order model (up to order $n-1$) was accepted if AIC decreased > 3 units and the p -value for the mean did not decrease.

F.3.3. Model Selection

After fitting these models to the data sets, the recommendations for model selection set out in U.S. EPA's *Benchmark Dose Technical Guidance Document* (External Review Draft, [\(U.S. EPA, 2000b\)](#)) were applied. First, models were generally rejected if the p -value for goodness of fit was < 0.10 . In a few cases in which none of the models fit the data with $p > 0.10$, linear models were selected on the basis of an adequate visual fit overall. Second, models were rejected if they did not appear to adequately fit the low-dose region of the dose-response relationship, based on an examination of graphical displays of the data and scaled residuals. If the BMDL estimates from the remaining models were "sufficiently close" (a criterion of within twofold for "sufficiently close" was used), then the model with the lowest AIC was selected. The AIC is a measure of information loss from a dose-response model that can be used to compare a set of models. Among a specified set of models, the model with the lowest AIC is considered the "best." If two or more models share the lowest AIC, the draft *Benchmark Dose*

Technical Guidance Document ([U.S. EPA, 2000b](#)) suggests that an average of the BMDLs could be used, but averaging was not used in this assessment (for the one occasion in which models shared the lowest AIC, a selection was made based on visual fit). If the BMDL estimates from the remaining models are not sufficiently close, some model dependence is assumed. With no clear biological or statistical basis to choose among them, the lowest BMDL was chosen as a reasonable conservative estimate, as suggested in the draft *Benchmark Dose Technical Guidance Document*, unless the lowest BMDL appeared to be an outlier, in which case further judgments were made.

F.3.4. Additional Adjustments for Selected Data Sets

In a few cases, the dose-response data necessitated further adjustments in order to improve model fits.

The behavioral/neurological endpoint “number of rears” from Moser et al. ([1995](#)) consisted of counts, measured at five doses and four measurement times (with eight observations each). The high dose for this endpoint was dropped because the mean was zero, and no monotone model could fit that well. Analysis of means and SDs for these counts suggested a Box-Cox power transform ([Box et al., 1978](#)) of 0.5 (i.e., square root) to stabilize variances (i.e., the slope of the regression of log[SD] on log[mean] was 0.46, and the relation was linear and highly significant). This information was helpful in selecting a suitable variance model with high confidence (i.e., variance constant, for square-root transformed data). Thus, the square root was taken of the original individual count data, and the mean and variance of the transformed count data were used in the BMD modeling.

The high-dose group was dropped due to supra-linear dose-response shapes in two cases: fetal cardiac malformations from Johnson et al. ([2003](#)) and decreased PFC response from Woolhiser et al. ([2006](#)). Johnson et al. ([2003](#)) is discussed in more detail below (see Section F.4.2.1). For Woolhiser et al. ([2006](#)), model fit near the BMD and the lower doses as well as the model fit to the variance were improved by dropping the highest dose, a procedure suggested in U.S. EPA ([2000b](#)).

In some cases, the supralinear dose-response shape could not be accommodated by these measures, and a LOAEL or NOAEL was used instead. These include NCI ([1976](#)) (toxic nephrosis, >90% response at lowest dose), Keil ([2009](#)) (autoimmune markers and decreased thymus weight, only two dose groups in addition to controls), and Peden-Adams et al. ([2006](#)) (developmental immunotoxicity, only two dose groups in addition to controls).

F.4. DOSE-RESPONSE MODELING RESULTS

F.4.1. Quantal Dichotomous and Continuous Modeling Results

Supplementary data files show the fitted model curves ("[Supplementary data for TCE assessment: Non-cancer plots contin,](#)" 2011; "[Supplementary data for TCE assessment: Non-](#)

[cancer plots dichot," 2011](#)). The graphics include observations (group means or proportions), the estimated model curve (solid red line), and estimated BMD, with a BMDL. Vertical bars show 95% CIs for the observed means. Printed above each plot are some key statistics (necessarily rounded) for model goodness of fit and estimated parameters. Printed in the plots in the upper left are the BMD and BMDL for the rodent data, in the same units as the rodent dose.

More detailed results, including alternative BMRs, alternative dose-metrics, quantal analyses for endpoints for which nested analyses were performed, etc. are documented in the several spreadsheets. Input data for the analyses are in other supplementary data files (["Supplementary data for TCE assessment: Non-cancer input data contin," 2011](#); ["Supplementary data for TCE assessment: Non-cancer input data dichot," 2011](#)). Additional supplementary data files (["Supplementary data for TCE assessment: Non-cancer results contin," 2011](#); ["Supplementary data for TCE assessment: Non-cancer results dichot," 2011](#)) present the data and model summary statistics, including goodness-of-fit measures (χ^2 goodness-of-fit p -value, AIC), parameter estimates, BMD, and BMDL. The group numbers "GRP" are arbitrary and are the same as GRP in the plots. Finally, note that not all plots are shown in the documents above, since these spreadsheets include many "alternative" analyses.

F.4.2. Nested Dichotomous Modeling Results

F.4.2.1. Johnson et al. (2003) Fetal Cardiac Defects

F.4.2.1.1. Results using applied dose.

The biological endpoint was frequency of rat fetuses having cardiac defects, as shown in Table F-4. Individual animal data were kindly provided by Dr. Johnson ([personal communication from Paula Johnson, University of Arizona, to Susan Makris, U.S. EPA, 26 August 2009](#)). Cochran-Armitage trend tests using number of fetuses and number of litters indicated significant increases in response with dose (with or without including the highest dose).

One suitable candidate for a LSC was available: female weight gain during pregnancy. Based on goodness of fit, this covariate did not contribute to better fit and was not used. Some ICs were significant and these parameters were included in the model.

Table F-4. Data on fetuses and litters with abnormal hearts from Johnson et al. (2003)

Dose group (mg/kg/d):	0	0.00045	0.048	0.218	129
Fetuses					
Number of pups:	606	144	110	181	105
Abnormal heart:	13	0	5	9	11
Litters					
Number of litters:	55	12	9	13	9
Abnormal heart:	9	0	4	5	6

With the high dose included, the χ^2 goodness of fit was acceptable, but some residuals were large (1.5 to 2) for the control and two lower doses. Therefore, models were also fitted after dropping the highest dose. For these, goodness of fit was adequate, and scaled residuals were smaller for the low doses and control. Predicted expected response values were closer to observed when the high dose was dropped, as shown in Table F-5:

Table F-5. Comparison of observed and predicted numbers of fetuses with abnormal hearts from Johnson et al. (2003), with and without the high-dose group, using a nested model

Dose group (mg/kg/d):	Abnormal hearts (pups)				
	0	0.00045	0.048	0.218	129
Observed:	13	0	5	9	11
Predicted expected:					
With high dose	19.3	4.5	3.5	5.7	11
Without high dose	13.9	3.3	3.4	10	–

Accuracy in the low-dose range is especially important because the BMD is based upon the predicted responses at the control and the lower doses. Based on the foregoing measures of goodness of fit, the model based on dropping the high dose was used.

The nested log-logistic and Rai-VanRyzin models were fitted; these gave essentially the same predicted responses and POD. The former model was used as the basis for a POD; results are in Table F-6 and Figure F-2.

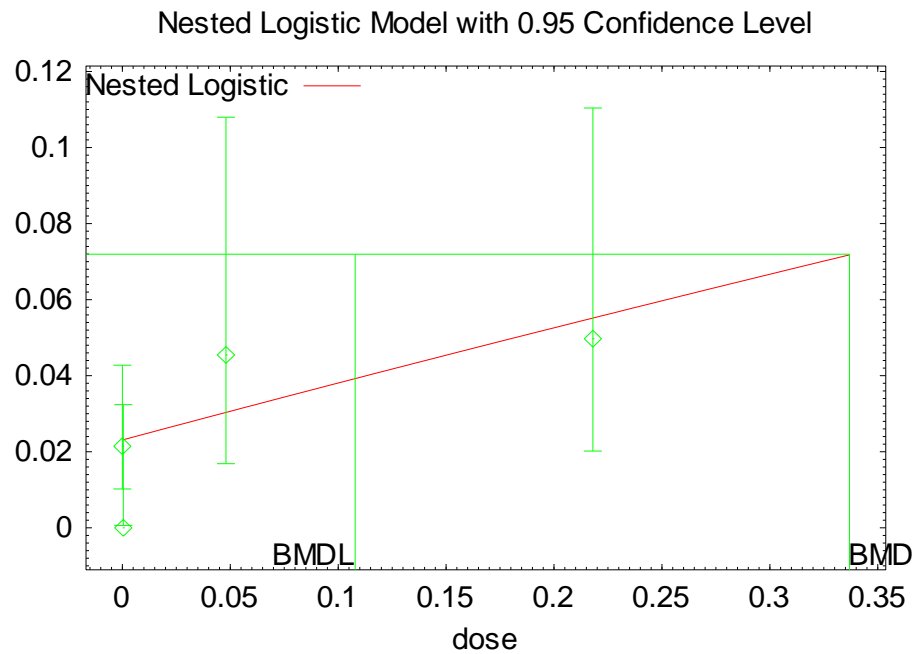
Table F-6. Results of nested log-logistic model for fetal cardiac anomalies from Johnson et al. (2003) without the high-dose group, on the basis of applied dose (mg/kg/day in drinking water)

Model	LSC? ^a	IC?	AIC	Pval	BMR	BMD	BMDL
NLOG	Y	Y	246.877	NA (df = 0)	0.01	0.252433	0.03776
NLOG	Y	N	251.203	0.0112	0.01	0.238776	0.039285
NLOG	N	N	248.853	0.0098	0.01	0.057807	0.028977
NLOG	N	Y	243.815	0.0128	0.1	0.71114	0.227675
NLOG	N	Y	243.815	0.0128	0.05	0.336856	0.107846
NLOG^b	N	Y	243.815	0.0128	0.01	0.064649	0.020698

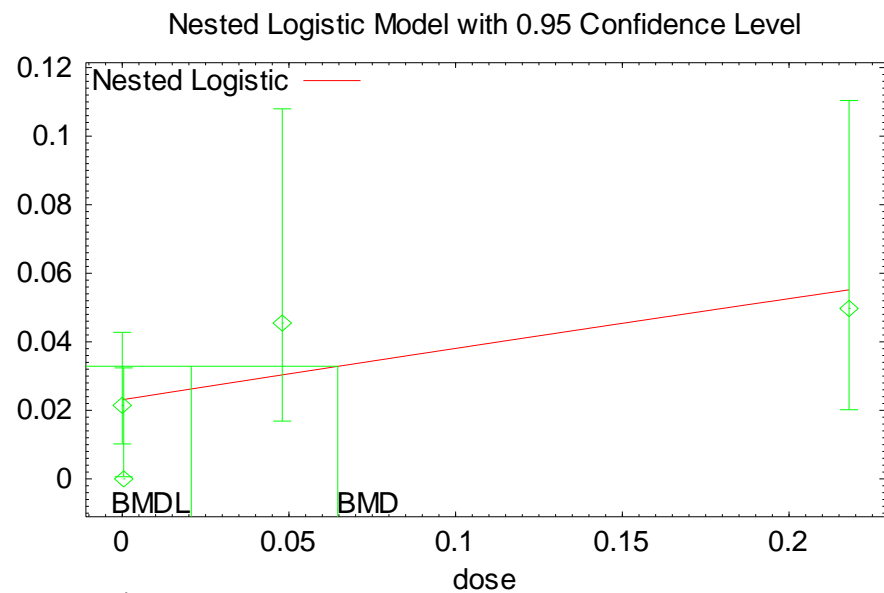
^aLSC analyzed was female weight gain during pregnancy.

^bIndicates model selected (Rai-VanRyzin model fits are essentially the same).

NLOG = “nested log-logistic” model



13:36 08/27 2008



13:37 08/27 2008

Figure F-2. BMD modeling of Johnson et al. (2003) using nested log-logistic model, with applied dose, without LSC, with IC, and without the high-dose group, using a BMR of 0.05 extra risk (top panel) or 0.01 extra risk (bottom panel).

F.4.2.1.2. χ^2 Goodness-of-Fit Test for nested log-logistic model.

The BMDS choice of subgroups did not seem appropriate given the data. The high-dose group of 13 litters was subdivided into three subgroups having sums of expected counts 3, 3, and 2. However, the control group of 55 litters could have been subdivided because expected

response rates for controls were relatively high. There was also concern that the goodness of fit might change with alternative choices of subgroupings.

An R program was written to read the BMDS output, reading parameters and the table of litter-specific results (dose, covariate, estimated probability of response, litter size, expected response count, observed response count, scaled χ^2 residual). The control group of 55 litters was subdivided into three subgroups of 18, 18, and 19 litters. Control litters were sampled randomly without replacement 100 times, each time creating 3 subgroups (i.e., 100 random assignments of the 55 control litters to three subgroups were made). For each of these, the goodness-of-fit calculation was made and the *p*-value saved. Within these 100 *p*-values, $\geq 75\%$ were ≥ 0.05 and $\geq 50\%$ had *p*-values ≥ 0.11 ; this indicated that the model is acceptable based on goodness-of-fit criteria.

F.4.2.1.3. Results using PBPK model-based dose-metrics.

The nested log-logistic model was also run using the dose-metrics in the dams of total oxidative metabolism scaled by body weight to the $3/4$ -power (TotOxMetabBW34) and the AUC of TCE in blood (AUCCBld). As with the applied dose modeling, LSC (maternal weight gain) was not included, but IC was included, based on the criteria outlined previously (see Section F.3.1.2). The results are summarized in Table F-7 and Figure F-3 for TotOxMetabBW34 and Table F-8 and Figure F-4 for AUCCBld.

Table F-7. Results of nested log-logistic model for fetal cardiac anomalies from Johnson et al. (2003) without the high-dose group, using the TotOxMetabBW34 dose-metric

Model	LSC? ^a	IC?	AIC	Pval	BMR	BMD	BMDL
NLOG	Y	Y	246.877	NA (df = 0)	0.01	0.174253	0.0259884
NLOG	Y	N	251.203	0.0112	0.01	0.164902	0.0270378
NLOG	N	Y	243.815	0.0128	0.1	0.489442	0.156698
NLOG^b	N	Y	243.815	0.0128	0.01	0.0444948	0.0142453
NLOG	N	N	248.853	0.0098	0.01	0.0397876	0.0199438

^aLSC analyzed was female weight gain during pregnancy.

^bIndicates model selected. BMDS failed with the Rai-VanRyzin and NCTR models.

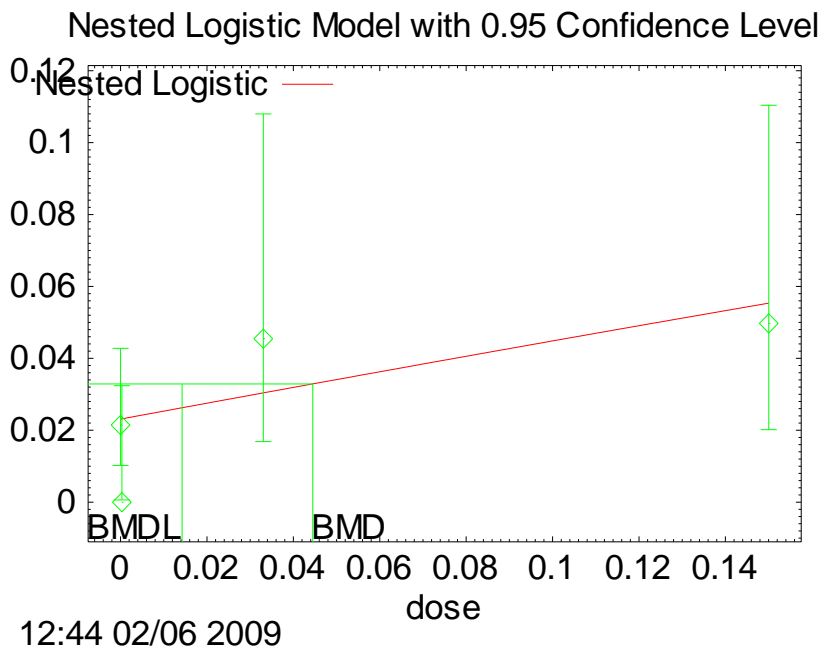


Figure F-3. BMD modeling of Johnson et al. (2003) using nested log-logistic model, with TotOxMetabBW34 dose-metric, without LSC, with IC, and without the high-dose group, using a BMR of 0.01 extra risk.

Table F-8. Results of nested log-logistic model for fetal cardiac anomalies from Johnson et al. (2003) without the high-dose group, using the AUCCBld dose-metric

Model	LSC? ^a	IC?	AIC	Pval	BMR	BMD	BMDL
NLOG	Y	Y	246.877	NA (df = 0)	0.01	0.00793783	0.00118286
NLOG	Y	N	251.203	0.0112	0.01	0.00750874	0.00123047
NLOG ^b	N	Y	243.816	0.0128	0.1	0.0222789	0.00712997
NLOG^b	N	Y	243.816	0.0128	0.01	0.00202535	0.000648179
NLOG	N	N	248.853	0.0098	0.01	0.00181058	0.000907513

^aLSC analyzed was female weight gain during pregnancy.

^bIndicates model selected. BMDS failed with the Rai-VanRyzin and NCTR models.

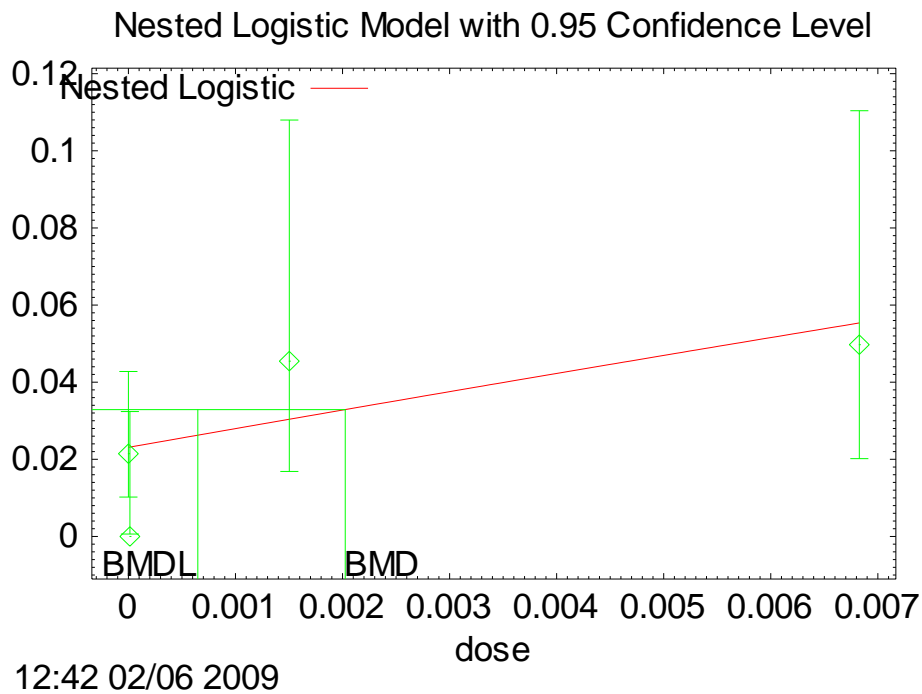


Figure F-4. BMD modeling of Johnson et al. (2003) using nested log-logistic model, with AUCCBld dose-metric, without LSC, with IC, and without the high-dose group, using a BMR of 0.01 extra risk.

F.4.2.2. Narotsky et al. (1995)

Data were combined for the high doses in the single-agent experiment and the lower doses in the ‘five-cube’ experiment. Individual animal data were kindly provided by Dr. Narotsky ([personal communications from Michael Narotsky, U.S. EPA, to John Fox, U.S. EPA, 19 June 2008, and to Jennifer Jinot, U.S. EPA, 10 June 2008](#)). Two endpoints were examined: frequency of eye defects in rat pups and prenatal loss (number of implantation sites minus number of live pups on PND 1).

Two LSCs were considered, with analyses summarized in Table F-9. The number of implants is unrelated to dose, as inferred from regression and ANOVA, and was considered as a LSC for eye defects. As number of implants is part of the definition for the endpoint of prenatal loss, it is not considered as a LSC for prenatal loss. A second LSC, the dam body weight on GD 6 (damBW6) was significantly related to dose and is unsuitable as a litter-specific covariate.

Table F-9. Analysis of LSCs with respect to dose from Narotsky et al. (1995)

Relation of litter-specific covariates to dose			
Implants:	none		
damBW6:	significant		
		Mean	Mean
	TCE	Implants	damBW6
	0	9.5	176.0
	10.1	10.1	180.9
	32	9.1	174.9
	101	7.8	170.1
	320	10.4	174.5
	475	9.7	182.4
	633	9.6	185.3
	844	8.9	182.9
	1,125	9.6	184.2
Using expt as covariate, e.g., damBW6 ~ TCE.mg.kgd + expt			
Linear regression		$p = 0.7486$	$p = 0.0069$
AoV (ordered factor)		$p = 0.1782$	$p = 0.0927$

Two LSCs were considered, with analyses summarized in Table F-9. The number of implants is unrelated to dose, as inferred from regression and ANOVA, and was considered as a LSC for eye defects. As number of implants is part of the definition for the endpoint of prenatal loss, it is not considered as a LSC for prenatal loss. A second LSC, the dam body weight on GD 6 (damBW6) was significantly related to dose and is unsuitable as a litter-specific covariate.

F.4.2.2.1. Fetal eye defects

The nested log-logistic and Rai-VanRyzin models were fitted to the number of pups with eye defects reported by Narotsky et al. (1995), with the results summarized in Table F-10.

Table F-10. Results of nested log-logistic and Rai-VanRyzin model for fetal eye defects from Narotsky et al. (1995), on the basis of applied dose (mg/kg/day in drinking water)

Model	LSC? ^a	IC?	AIC	Pval	BMR	BMD	BMDL
NLOG	Y	Y	255.771	0.3489	0.05	875.347	737.328 ^b
NLOG	Y	N	259.024	0.0445	0.05	830.511	661.629
NLOG	N	Y	270.407	0.2281	0.05	622.342	206.460
NLOG	N	N	262.784	0.0529	0.10	691.93	542.101
NLOG	N	N	262.784	0.0529	0.05	427.389	264.386
NLOG	N	N	262.784	0.0529	0.01	147.41	38.7117 ^c
RAI	Y	Y	274.339	0.1047	0.05	619.849	309.925
RAI	Y	N	264.899	0.0577	0.05	404.788	354.961
RAI	N	Y	270.339	0.2309	0.05	619.882	309.941
RAI	N	N	262.481	0.0619	0.10	693.04	346.52
RAI	N	N	262.481	0.0619	0.05	429.686	214.843
RAI	N	N	262.481	0.0619	0.01	145.563	130.938 ^c

^aLSC analyzed was implants.

^bGraphical fit at the origin exceeds observed control and low-dose responses and slope is quite flat (see Figure F-5), fitted curve does not represent the data well.

^cIndicates model selected.

RAI = Rai-VanRyzin model

Results for the nested log-logistic model suggested a better model fit with the inclusion of the LSC and IC, based on AIC. However, the graphical fit (see Figure F-5) is strongly sublinear and high at the origin where the fitted response exceeds the observed low-dose responses for the control group and two low-dose groups. An alternative nested log-logistic model without either LSC or IC (see Figure F-6), which fits the low-dose responses better, was selected. Given that this model had no LSC and no IC, the nested log-logistic model reduces to a quantal log-logistic model. Parameter estimates and the *p*-values were essentially the same for the two models (see Table F-11). A similar model selection can be justified for the Rai-Van Ryzin model (see Figure F-7). Because no LSC and no IC were needed, this endpoint was modeled with quantal models, using totals of implants and losses for each dose group, which allowed choice from a wider range of models (those results appear with quantal model results in this appendix).

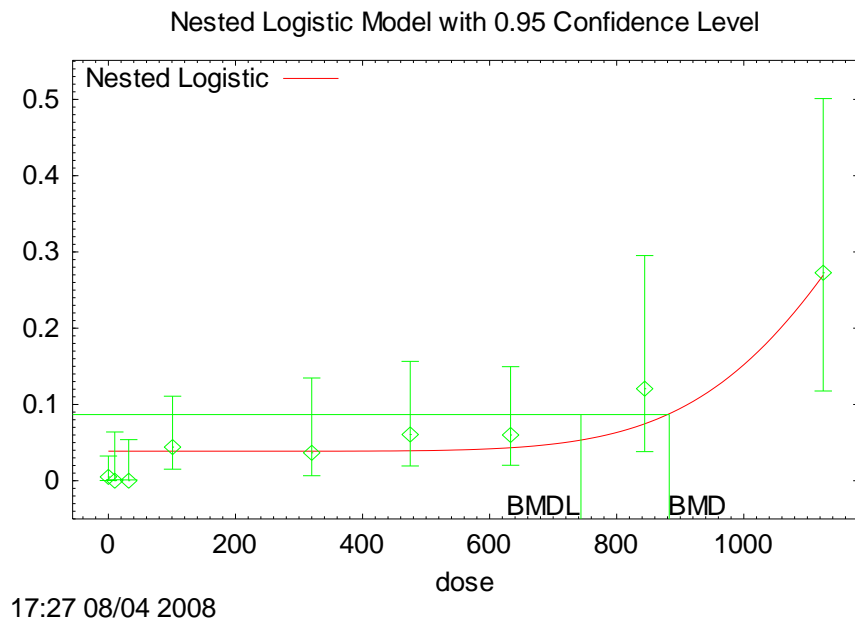


Figure F-5. BMD modeling of fetal eye defects from Narotsky et al. (1995) using nested log-logistic model, with applied dose, with both LSC and IC, using a BMR of 0.05 extra risk.

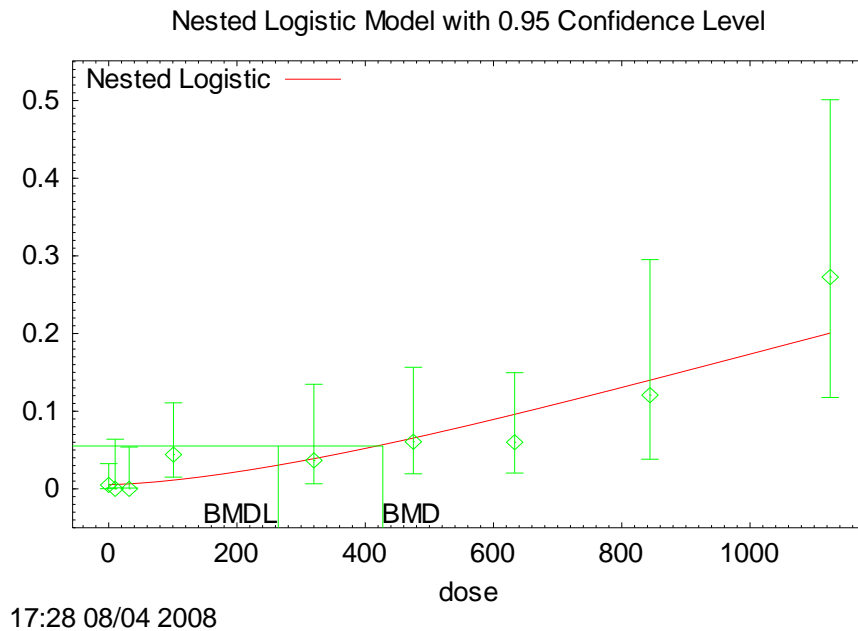


Figure F-6. BMD modeling of fetal eye defects from Narotsky et al. (1995) using nested log-logistic model, with applied dose, without either LSC or IC, using a BMR of 0.05 extra risk.

Table F-11. Comparison of results of nested log-logistic (without LSC or IC) and quantal log-logistic model for fetal eye defects from Narotsky et al. (1995)

Model	Parameter			BMD ₀₅	BMDL ₀₅
	Alpha	Beta	Rho		
Nested	0.00550062	-12.3392	1.55088	427.4	264.4
Quantal	0.00549976	-12.3386	1.55079	427.4	260.2

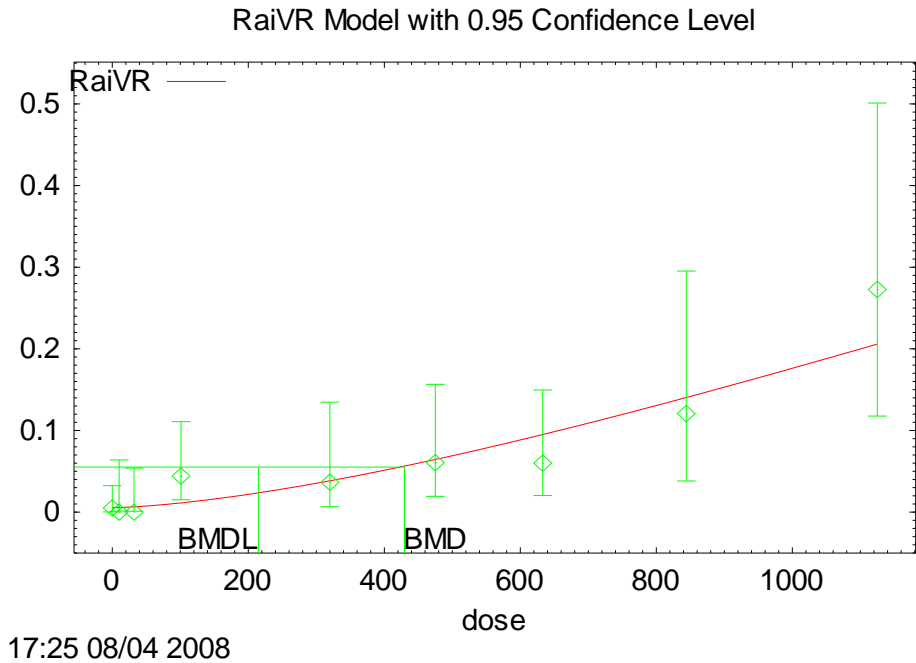


Figure F-7. BMD modeling of fetal eye defects from Narotsky et al. (1995) using nested Rai-VanRyzin model, with applied dose, without either LSC or IC, using a BMR of 0.05 extra risk.

F.4.2.2.2. Narotsky et al. (1995) prenatal loss

The nested log-logistic and Rai-VanRyzin models were fitted to prenatal loss reported by Narotsky et al. (1995), with the results summarized in Table F-12.

Table F-12. Results of nested log-logistic and Rai-VanRyzin model for prenatal loss from Narotsky et al. (1995), on the basis of applied dose (mg/kg/day in drinking water)

Model	LSC? ^a	IC?	AIC	Pval	BMR	BMD	BMDL
NLOG	Y	Y	494.489	0.2314	0.10	799.723	539.094
NLOG	Y	N	627.341	0.0000	0.10	790.96	694.673
NLOG	N	N	628.158	0.0000	0.10	812.92	725.928
NLOG	N	Y	490.766	0.2509	0.10	814.781	572.057
NLOG	N	Y	490.766	0.2509	0.05	738.749	447.077
NLOG	N	Y	490.766	0.2509	0.01	594.995	252.437^b
RAI	Y	Y	491.859	0.3044	0.10	802.871	669.059
RAI	Y	N	626.776	0.0000	0.10	819.972	683.31
RAI	N	N	626.456	0.0000	0.10	814.98	424.469
RAI	N	Y	488.856	0.2983	0.10	814.048	678.373
RAI	N	Y	488.856	0.2983	0.05	726.882	605.735
RAI	N	Y	488.856	0.2983	0.01	562.455	468.713^b

^aLSC analyzed was dam body weight on GD 6.

^bIndicates model selected.

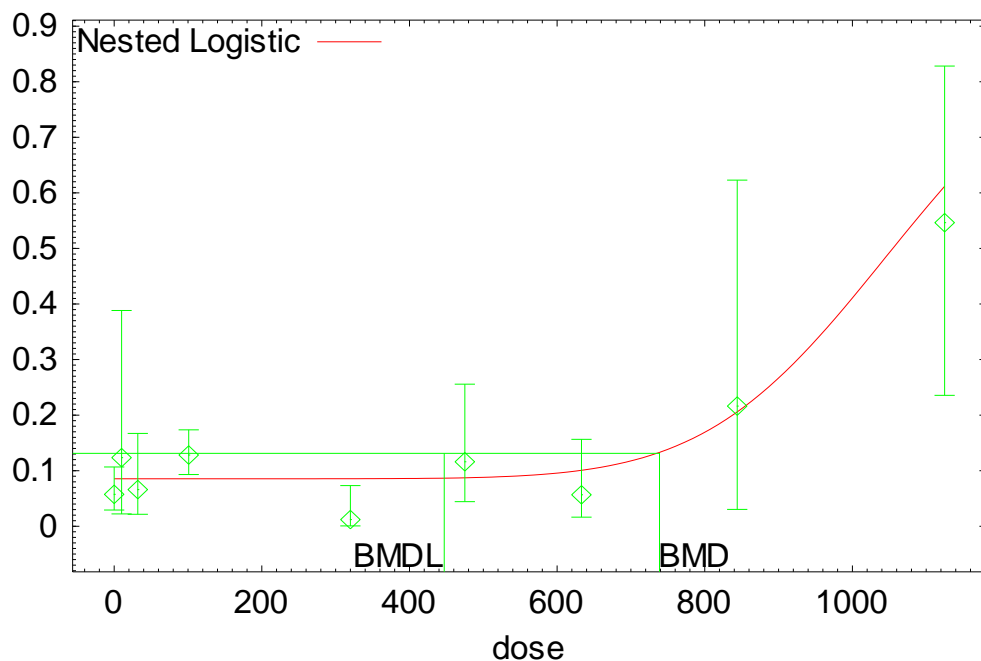
The BMDS nested models require a LSC, so dam body weight on GD6 (“damBW6”) was used as the LSC. However, damBW6 is significantly related to dose and, so, is not a reliable LSC. Number of implants could not be used as a LSC because it was identified as number at risk in the BMDS models. These issues were obviated because the model selected did not employ the LSC.

For the nested log-logistic models, the AIC is much larger when the IC is dropped, so the IC is needed in the model. The LSC can be dropped (and is also suspect because it is correlated with dose). The model with IC and without LSC was selected on the basis of AIC (shown in Figure F-8). For the Rai-VanRyzin models, the model selection was similar to that for the nested log-logistic, leading to a model with IC and without LSC, which had the lowest AIC (shown in Figure F-9).

F.4.3. Model Selections and Results

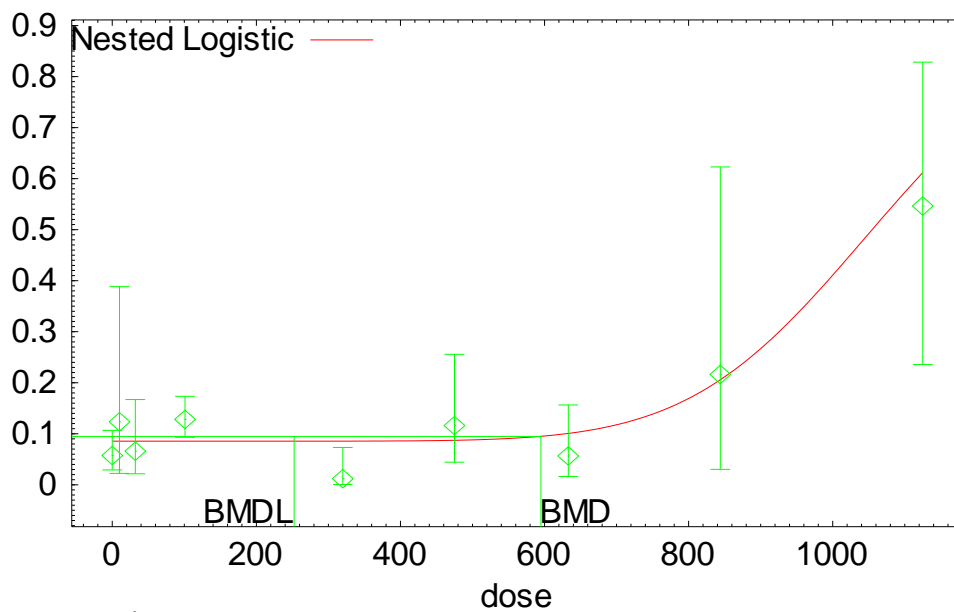
The final model selections and results for noncancer dose-response modeling are presented in Table F-13.

Nested Logistic Model with 0.95 Confidence Level



16:44 08/20 2008

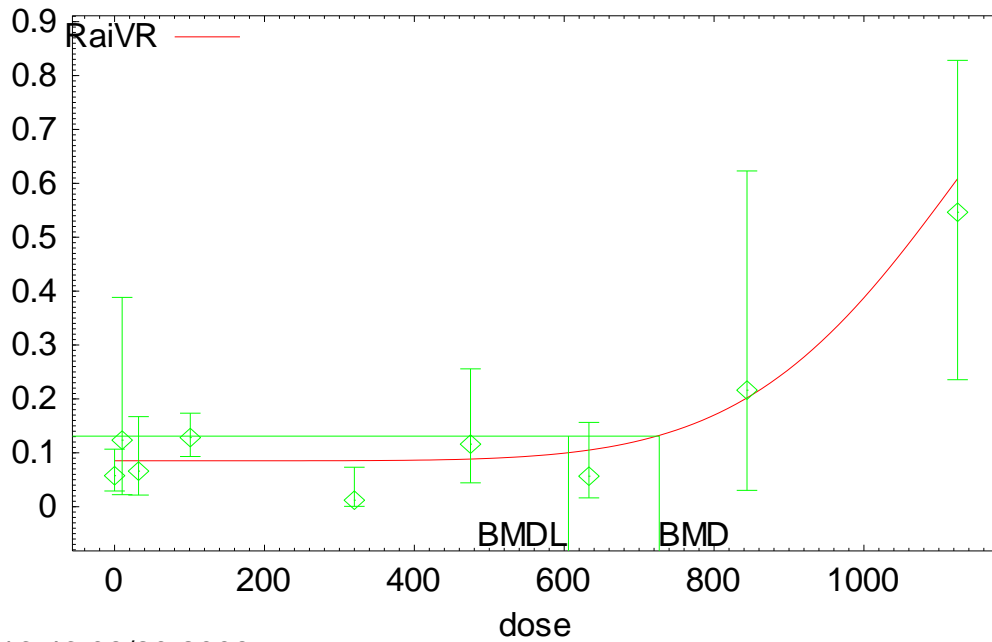
Nested Logistic Model with 0.95 Confidence Level



16:45 08/20 2008

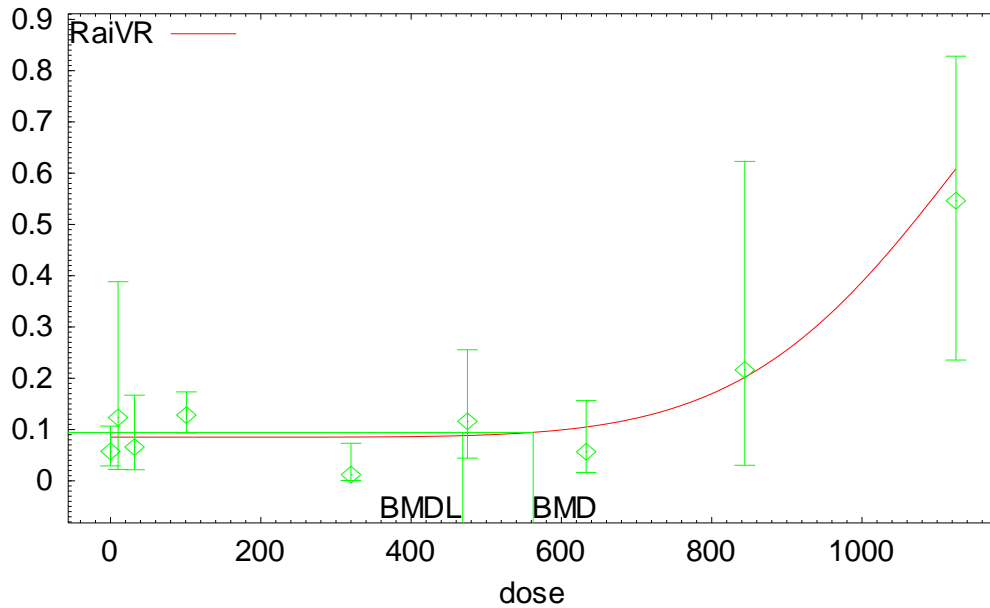
Figure F-8. BMD modeling of prenatal loss reported in Narotsky et al. (1995) using nested log-logistic model, with applied dose, without LSC, with IC, using a BMR of 0.05 extra risk (top panel) or 0.01 extra risk (bottom panel).

RaiVR Model with 0.95 Confidence Level



16:46 08/20 2008

RaiVR Model with 0.95 Confidence Level



16:46 08/20 2008

Figure F-9. BMD modeling of prenatal loss reported in Narotsky et al. (1995) using nested Rai-VanRyzin model, with applied dose, without LSC, with IC, using a BMR of 0.05 extra risk (top panel) or 0.01 extra risk (bottom panel).

Table F-13. Model selections and results for noncancer dose-response analyses

GRP	Study/run abbrev.	Species	Sex	Strain	Exposure route	Endpoint	Dose-metric	BMR type	BM R	BMD/ BMD L	BMDL	Model	Rep. BMD	Notes
Dichotomous models														
3	Chia et al. (1996)	Human	M	workers.elec.factory	inhal	N.hyperzoospermia	appl.dose	extra	0.1	2.14	1.43	loglogistic.1	3.06	
7	Narotsky et al. (1995)	Rat	F	F344	oral.gav	N.pups.eye.defects	appl.dose	extra	0.01	1.46	60.1	multistage	806	a
13	Narotsky et al. (1995)	Rat	F	F344	oral.gav	N.dams.w.resorbed.litters	appl.dose	extra	0.01	5.47	32.2	multistage.2	570	
13	Narotsky et al. (1995)	Rat	F	F344	oral.gav	N.dams.w.resorbed.litters	AUCCBld	extra	0.01	5.77	17.5	multistage.2	327	
13	Narotsky et al. (1995)	Rat	F	F344	oral.gav	N.dams.w.resorbed.litters	TotMetabBW34	extra	0.01	1.77	77.5	weibull	156	
14	Johnson et al. (2003).drophi	Rat	F	Sprague.Dawley	oral.dw	N.litters.abnormal.hearts	appl.dose	extra	0.1	2.78	0.0146	loglogistic.1	0.0406	b
36	Griffin et al. (2000b)	mice	F	MRL++	oral.dw	portal.infiltration	appl.dose	extra	0.1	2.67	13.4	loglogistic.1	35.8	
38	Maltoni et al. (1986)	Rat	M	Sprague.Dawley	inhal	megalonucleocytosis	appl.dose	extra	0.1	1.22	40.2	multistage	49.2	c
38	Maltoni et al. (1986)	Rat	M	Sprague.Dawley	inhal	megalonucleocytosis	ABioactDCVCBW34	extra	0.1	1.18	0.0888	loglogistic	0.105	
38	Maltoni et al. (1986)	Rat	M	Sprague.Dawley	inhal	megalonucleocytosis	AMetGSHBW34	extra	0.1	1.19	0.086	loglogistic	0.102	
38	Maltoni et al. (1986)	Rat	M	Sprague.Dawley	inhal	megalonucleocytosis	TotMetabBW34	extra	0.1	1.13	53.8	weibull	61	d
39	Maltoni et al. (1986)	Rat	M	Sprague.Dawley	oral.gav	megalonucleocytosis	appl.dose	extra	0.1	1.53	33.8	multistage.2	51.8	e
39	Maltoni et al. (1986)	Rat	M	Sprague.Dawley	oral.gav	megalonucleocytosis	ABioactDCVCBW34	extra	0.1	1.60	0.0594	multistage.2	0.0948	
39	Maltoni et al. (1986)	Rat	M	Sprague.Dawley	oral.gav	megalonucleocytosis	AMetGSHBW34	extra	0.1	1.65	0.0605	multistage.2	0.0977	
39	Maltoni et al. (1986)	Rat	M	Sprague.Dawley	oral.gav	megalonucleocytosis	TotMetabBW34	extra	0.1	1.41	20.5	multistage.2	29	e
49	NTP (1988)	Rat	F	Marshall	oral.gav	toxic nephropathy	appl.dose	extra	0.05	1.45	9.45	loglogistic.1	28.9	
49	NTP (1988)	Rat	F	Marshall	oral.gav	toxic nephropathy	ABioactDCVCBW34	extra	0.05	1.45	0.0132	loglogistic.1	0.0404	
49	NTP (1988)	Rat	F	Marshall	oral.gav	toxic nephropathy	AMetGSHBW34	extra	0.05	1.46	0.0129	loglogistic.1	0.0397	
49	NTP (1988)	Rat	F	Marshall	oral.gav	toxic nephropathy	TotMetabBW34	extra	0.05	1.45	2.13	loglogistic.1	6.5	

Table F-13. Model selections and results for noncancer dose-response analyses (continued)

GRP	Study/run abbrev.	Species	Sex	Strain	Exp. route	Endpoint	Dose-metric	BMR type	BM R	BMD/BMD L	BMDL	Model	Rep. BMD	Notes
Nested dichotomous models														
NA	Johnson et al. (2003).drophi	rat	F	Sprague.Dawley	oral.dw	N.pups.abnormal.hearts	appl.dose	extra	0.01	3.12	0.0207	loglogistic.IC	0.711	b
NA	Johnson et al. (2003).drophi	rat	F	Sprague.Dawley	oral.dw	N.pups.abnormal.hearts	TotOxMetabBW34	extra	0.01	3.12	0.0142	loglogistic.IC		b
NA	Johnson et al. (2003).drophi	rat	F	Sprague.Dawley	oral.dw	N.pups.abnormal.hearts	AUCCBld	extra	0.01	3.12	0.000648	loglogistic.IC		b
NA	Narotsky et al. (1995)	rat	F	F344	oral.gav	N.prenatal.loss	appl.dose	extra	0.01	1.2	469	RAI.IC	814	
Continuous models														
2	Land et al. (1981)	mouse	M	(C57B1xC3H)F1	inhal	pct.abnormal.sperm	appl.dose	standard	0.5	1.33	46.9	polynomial.constvar	125	
6	Carney et al. (2006)	rat	F	Sprague-Dawley (CrI:CD)	inhal	gm.wgt.gain.GD6.9	appl.dose	relative	0.1	2.5	10.5	hill	62.3	
8	Narotsky et al. (1995)	rat	F	F344	oral.gav	gm.wgt.gain.GD6.20	appl.dose	relative	0.1	1.11	108	polynomial.constvar	312	
19	Crofton and Zhao (1997)	rat	M	Long-Evans	inhal	dB.auditory.threshold(16kHz)	appl.dose	absolute	10	1.11	274	polynomial.constvar	330	
21	George et al. (1986)	rat	F	F344	oral.food	litters	appl.dose	standard	0.5	1.69	179	polynomial.constvar	604	
23	George et al. (1986)	rat	F	F344	oral.food	live.pups	appl.dose	standard	0.5	1.55	152	polynomial.constvar	470	
26	George et al. (1986)	rat	F	F344	oral.food	Foffspring.BWgm.day21	appl.dose	relative	0.05	1.41	79.7	polynomial.constvar	225	

Table F-13. Model selections and results for noncancer dose-response analyses (continued)

GRP	Study/run abbrev.	Species	Sex	Strain	Exp. route	Endpoint	Dose-metric	BMR type	BM R	BMD/BMD/L	BMDL	Model	Rep. BMD	Notes
34sq	Moser et al. (1995)+per scom	rat	F	F344	oral.gav	no.rears	appl.dose	standard	1	1.64	248	polynomial.constvar	406	b,f
49	George et al. (1986)	rat	F	F344	oral.food	traverse.time.21do	appl.dose	relative	1	1.98	72.6	power	84.9	
51	Buben and O'Flaherty (1985)	mouse	M	SwissCox	oral.gav	Liverwt.pctBW	appl.dose	relative	0.1	1.26	81.5	hill.constvar	92.8	
51	Buben and O'Flaherty (1985)	mouse	M	SwissCox	oral.gav	Liverwt.pctBW	AMetLiv1BW34	relative	0.1	1.08	28.6	polynomial.constvar	28.4	
51	Buben and O'Flaherty (1985)	mouse	M	SwissCox	oral.gav	Liverwt.pctBW	TotOxMetabBW34	relative	0.1	1.08	37	polynomial.constvar	36.7	
58	Kjellstrand et al. (1983a)	mouse	M	NMRI	inhal	Liverwt.pctBW	appl.dose	relative	0.1	1.36	21.6	hill	30.4	
58	Kjellstrand et al. (1983a)	mouse	M	NMRI	inhal	Liverwt.pctBW	AMetLiv1BW34	relative	0.1	1.4	22.7	hill	32.9	
58	Kjellstrand et al. (1983a)	mouse	M	NMRI	inhal	Liverwt.pctBW	TotOxMetabBW34	relative	0.1	1.3	73.4	hill	97.7	
60.Rp	Kjellstrand et al. (1983a)	mouse	M	NMRI	inhal	Kidneywt.pctBW	appl.dose	relative	0.1	1.17	34.7	polynomial	47.1	
60.Rp	Kjellstrand et al. (1983a)	mouse	M	NMRI	inhal	Kidneywt.pctBW	AMetGSHBW34	relative	0.1	1.18	0.17	polynomial	0.236	
60.Rp	Kjellstrand et al. (1983a)	mouse	M	NMRI	inhal	Kidneywt.pctBW	TotMetabBW34	relative	0.1	1.17	71	polynomial	95.2	
63	Woolhiser et al. (2006)	rat	F	CD (Sprague-Dawley)	inhal	Antibody.Forming Cells	appl.dose	standard	1	1.94	31.2	power.constvar	60.6	b
62	Woolhiser et al. (2006)	rat	F	CD (Sprague-Dawley)	inhal	Antibody.Forming Cells	AUCCBld	standard	1	1.44	149	polynomial	214	

Table F-13. Model selections and results for noncancer dose-response analyses (continued)

GRP	Study/run abbrev.	Species	Sex	Strain	Exp. route	Endpoint	Dose-metric	BMR type	BM R	BMD/BMD L	BMDL	Model	Rep. BMD	Notes
62	Woolhiser et al. (2006)	rat	F	CD (Sprague-Dawley)	inhal	Antibody.Forming Cells	TotMetabBW34	standard	1	1.5	40.8	polynomial	61.3	
65	Woolhiser et al. (2006)	rat	F	CD (Sprague-Dawley)	inhal	kidney.wt.per100gm	appl.dose	relative	0.1	4.29	15.7	hill.constvar	54.3	
65	Woolhiser et al. (2006)	rat	F	CD (Sprague-Dawley)	inhal	kidney.wt.per100gm	ABioactDCVCBW34	relative	0.1	4.27	0.0309	hill.constvar	0.103	
65	Woolhiser et al. (2006)	rat	F	CD (Sprague-Dawley)	inhal	kidney.wt.per100gm	AMetGSHBW34	relative	0.1	4.28	0.032	hill.constvar	0.107	
65	Woolhiser et al. (2006)	rat	F	CD (Sprague-Dawley)	inhal	kidney.wt.per100gm	TotMetabBW34	relative	0.1	1.47	40.8	polynomial.constvar	52.3	
67	Woolhiser et al. (2006)	rat	F	CD (Sprague-Dawley)	inhal	liver.wt.per100gm	appl.dose	relative	0.1	4.13	25.2	hill.constvar	70.3	
67	Woolhiser et al. (2006)	rat	F	CD (Sprague-Dawley)	inhal	liver.wt.per100gm	AMetLiv1BW34	relative	0.1	1.53	46	polynomial.constvar	56.1	
67	Woolhiser et al. (2006)	rat	F	CD (Sprague-Dawley)	inhal	liver.wt.per100gm	TotOxMetabBW34	relative	0.1	1.53	48.9	polynomial.constvar	59.8	

^aEight-stage multistage model.

^bDropped highest dose.

^cThree-stage multistage model.

^dWeibull selected over log-logistic with the same AIC on basis of visual fit (less extreme curvature).

^eSecond-order MS selected on basis of visual fit (less extreme curvature).

^fSquare-root transformation of original individual count data.

Applied dose BMDLs are in units of ppm in air for inhalation exposures and mg/kg/day for oral exposures. Internal dose BMDLs are in dose-metric units. Reporting BMD is BMD using a BMR of 0.1 extra risk for dichotomous models, and 1 control SD for continuous models.

Log-logistic = unconstrained log-logistic; log-logistic.1 = constrained log-logistic; multistage = multistage with #stages=dose groups-1; multistage.n = n-stage multistage; log-logistic.IC = nested log-logistic with IC, without LSC; RAI.IC = Rai-VanRyzin model with IC, without LSC; zzz.constvar = continuous model zzz with constant variance (otherwise variance is modeled).

Rep. = reporting

F.5. DERIVATION OF POINTS OF DEPARTURE

F.5.1. Applied Dose Points of Departure

For oral studies in rodents, the POD on the basis of applied dose in mg/kg/day was taken to be the BMDL, NOAEL, or LOAEL. NOAELs and LOAELs were adjusted for intermittent exposure to their equivalent continuous average daily exposure (for BMDLs, the adjustments were already performed prior to BMD modeling).

For inhalation studies in rodents, the POD on the basis of applied dose in ppm was taken to be the BMDL, NOAEL, or LOAEL. NOAELs and LOAELs were adjusted for intermittent exposure to their equivalent continuous average daily exposure (for BMDLs, the adjustments were already performed prior to BMD modeling). These adjusted concentrations are considered HECs, in accordance with U.S. EPA ([1994a](#)), as TCE is considered a Category 3 gas (systemically acting) and has a blood-air partition coefficient in rodents greater than that in humans.¹⁴

F.5.2. PBPK Model-Based Human Points of Departure

As discussed in Section 5.1.3, the PBPK model was used for simultaneous interspecies (for endpoints in rodent studies), intraspecies, and route-to-route extrapolation based on the estimates from the PBPK model of the internal dose points of departure (idPOD) for each candidate critical study/endpoints. The following supplementary data files contain figures showing the derivation of the HEDs and HECs for the median (50th percentile) and sensitive (99th percentile) individual from the (rodent or human) study idPOD. In each case, for a specific study/endpoint(s)/sex/species (in the figure main title), and for a particular dose-metric (Y-axis label), the horizontal line shows the original study idPOD (a BMDL, NOAEL, or LOAEL as noted) and where it intersects with the human 99th percentile (open square) or median (closed square) exposure-internal-dose relationship:

1. HECs from human inhalation studies (["Supplementary data for TCE assessment: Non-cancer HECs plots from human inhalation studies," 2011](#))
2. HECs from rodent inhalation studies (["Supplementary data for TCE assessment: Non-cancer HECs plots from rodent inhalation studies," 2011](#))
3. HECs from rodent oral studies (["Supplementary data for TCE assessment: Non-cancer HECs plots from rodent oral studies," 2011](#))
4. HEDs from human inhalation studies (["Supplementary data for TCE assessment: Non-cancer HEDs plots from human inhalation studies," 2011](#))
5. HEDs from rodent inhalation studies (["Supplementary data for TCE assessment: Non-cancer HEDs plots from rodent inhalation studies," 2011](#))

¹⁴ The posterior population median estimate for the TCE blood:air partition coefficient was 14 in the mouse [Table 3-37], 19 in the rat [Table 3-38], and 9.2 in the human [Table 3-39].

6. HEDs from rodent oral studies (["Supplementary data for TCE assessment: Non-cancer HEDs plots from rodent oral studies," 2011](#))

The original study internal doses are based on the median estimates from about 2,000 “study groups” (for rodent studies) or “individuals” (for human studies), and corresponding exposures for the human median and 99th percentiles were derived from a distribution of 2,000 “individuals.” In both cases, the distributions reflect combined uncertainty (in the population means and variances) and population variability.

In addition, as part of the uncertainty/variability analysis described in Section 5.1.4.2, the POD for studies/endpoints for which BMD modeling was done was replaced by the LOAEL or NOAEL. This was done to because there was no available tested software for performing BMD modeling in such a context and because of limitations in time and resources to develop such software. However, the relative degree of uncertainty/variability should be adequately captured in the use of the LOAEL or NOAEL. The graphical depiction of the HEC₉₉ or HED₉₉ using these alternative PODs is shown in the following supplementary data files:

1. HECs from rodent inhalation studies (["Supplementary data for TCE assessment: Non-cancer HECs altPOD plots from rodent inhalation studies," 2011](#))
2. HECs from rodent oral studies (["Supplementary data for TCE assessment: Non-cancer HECs altPOD plots from rodent oral studies," 2011](#))
3. HEDs from rodent inhalation studies (["Supplementary data for TCE assessment: Non-cancer HEDs altPOD plots from rodent inhalation studies," 2011](#))
4. HEDs from rodent oral studies (["Supplementary data for TCE assessment: Non-cancer HEDs altPOD plots from rodent oral studies," 2011](#))

F.6. SUMMARY OF POINTS OF DEPARTURE (PODs) FOR STUDIES AND EFFECTS SUPPORTING THE INHALATION RfC AND ORAL RfD

This section summarizes the selection and/or derivation of PODs from the critical and supporting studies and effects that support the inhalation RfC and oral RfD. In particular, for each endpoint, the following are described: dosimetry (adjustments of continuous exposure, PBPK dose-metrics), selection of BMR and BMD model (if BMD modeling was performed), and derivation of the HEC or dose for a sensitive individual (if PBPK modeling was used). Section 5.1.3.1 discusses the dose-metric selection for different endpoints.

F.6.1. NTP ([NTP, 1988](#))—BMD Modeling of Toxic Nephropathy in Rats

The supporting endpoint here is toxic nephropathy in female Marshall rats ([NTP, 1988](#)), which was the most sensitive sex/strain in this study, although the differences among different sex/strain combinations was not large (BMDLs differed by threefold or less).

F.6.1.1. Dosimetry and BMD Modeling

Rats were exposed to 500 or 1,000 mg/kg/day, 5 days/week, for 104 weeks. The primary dose-metric was selected to be average amount of DCVC bioactivated/kg^{3/4}/day, with median estimates from the PBPK model for the female Marshall rats in this study of 0.47 and 1.1.

Figure F-10 shows BMD modeling for the dichotomous models used (see Section F.5.1, above). The log-logistic model with slope constrained to ≥ 1 was selected because: (1) the log-logistic model with unconstrained slope yielded a slope estimate < 1 and (2) it had the lowest AIC.

The idPOD of 0.0132 mg DCVC bioactivated/kg^{3/4}/day was a BMDL for a BMR of 5% extra risk. This BMR was selected because toxic nephropathy is a clear toxic effect. This BMR required substantial extrapolation below the observed responses (about 60%); however, the response level seemed warranted for this type of effect and the ratio of the BMD to the BMDL was not large (1.56 for the selected model).

F.6.1.2. Derivation of HEC₉₉ and HED₉₉

The HEC₉₉ and HED₉₉ are the lower 99th percentiles for the continuous HEC and continuous human ingestion dose that lead to a human internal dose equal to the rodent idPOD. The derivation of the HEC₉₉ of 0.0056 ppm and HED₉₉ of 0.00338 mg/kg/day for the 99th percentile for uncertainty and variability are shown in Figure F-11. These values are used as this supporting effect's POD to which additional UFs are applied.

NTP.1988 kidney toxic nephropathy rat Marshall F oral.gav (GRP 49)
 BMR: 0.05 extra

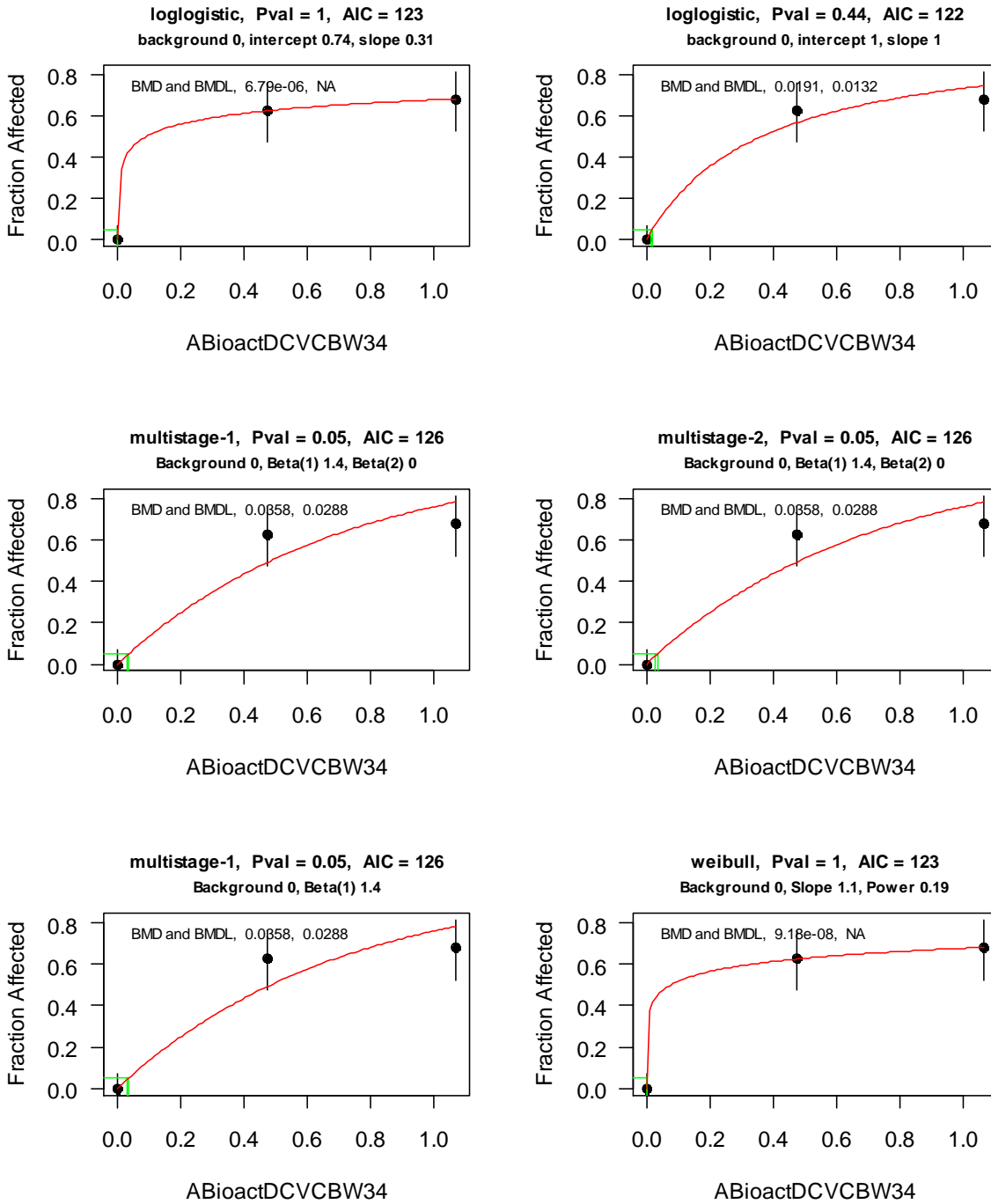


Figure F-10. BMD modeling of NTP (1988) toxic nephropathy in female Marshall rats.

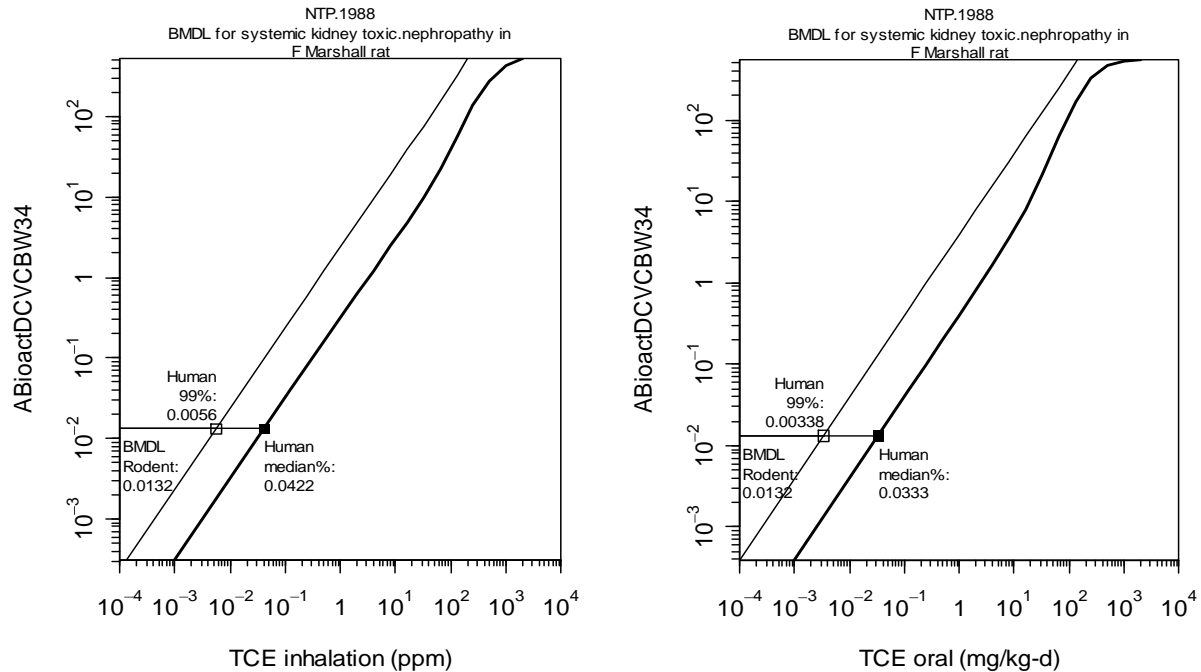


Figure F-11. Derivation of HEC₉₉ and HED₉₉ corresponding to the rodent idPOD from NTP (1988) toxic nephropathy in rats.

F.6.2. Woolhiser et al. (2006)—BMD Modeling of Increased Kidney Weight in Rats

The endpoint here is increased kidney weights in female Sprague-Dawley (Sprague-Dawley) rats (Woolhiser et al., 2006), which was considered a supporting effect for the RfD.

F.6.2.1. Dosimetry and BMD Modeling

Rats were exposed to 100, 300, and 1,000 ppm, 6 hours/day, 5 days/week, for 4 weeks. The primary dose-metric was selected to be average amount of DCVC bioactivated/kg^{3/4}/day, with median estimates from the PBPK model for this study of 0.038, 0.10, and 0.51.

Figure F-12 shows BMD modeling for the continuous models used (see Section F.5.2, above). The Hill model with constant variance was selected because it had the lowest AIC and because other models with the same AIC either were a power model with power parameter <1 or had poor fits to the control data set.

Woolhiser.etal.2006 Kidney kidney.wt.per100gm rat CD (Sprague-Dawley) F inhal (GRP 65)
 BMR: 0.1 relative

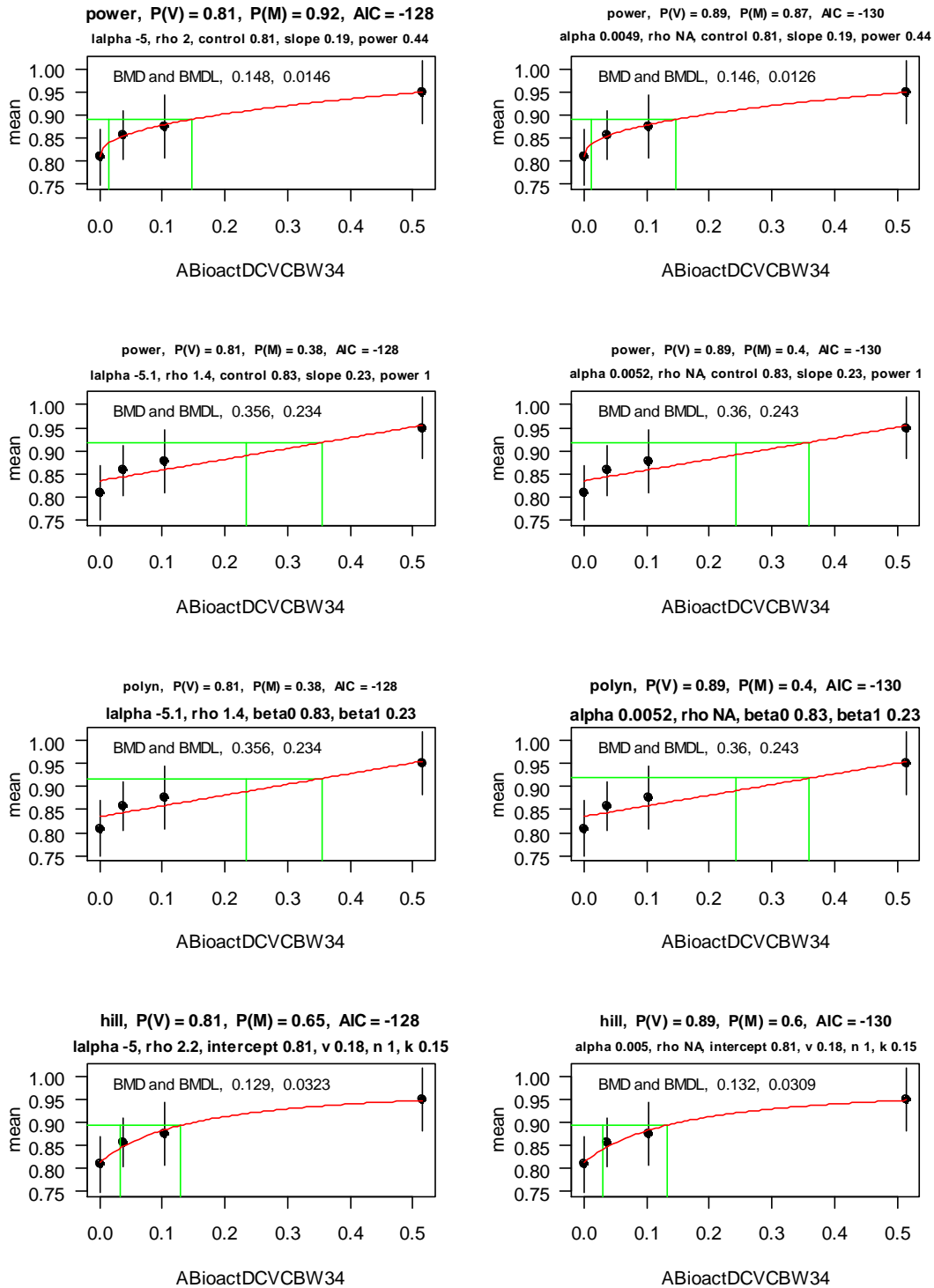


Figure F-12. BMD modeling of Woolhiser et al. (2006) for increased kidney weight in female Sprague-Dawley rats.

The idPOD of 0.0309 mg DCVC bioactivated/kg^{3/4}/day was a BMDL for a BMR of 10% weight change, which is the BMR typically used by U.S. EPA for body weight and organ weight changes. The response used in each case was the organ weight as a percentage of body weight, to account for any commensurate decreases in body weight, although the results did not differ much when absolute weights were used instead.

F.6.2.2. Derivation of HEC₉₉ and HED₉₉

The HEC₉₉ and HED₉₉ are the lower 99th percentiles for the continuous HEC and continuous human ingestion dose that lead to a human internal dose equal to the rodent idPOD. The derivation of the HEC₉₉ of 0.0131 ppm and HED₉₉ of 0.00791 mg/kg/day for the 99th percentile for uncertainty and variability are shown in Figure F-13. These values are used as this effect's POD to which additional UFs are applied, and the resulting candidate RfD value is supportive of the RfD.

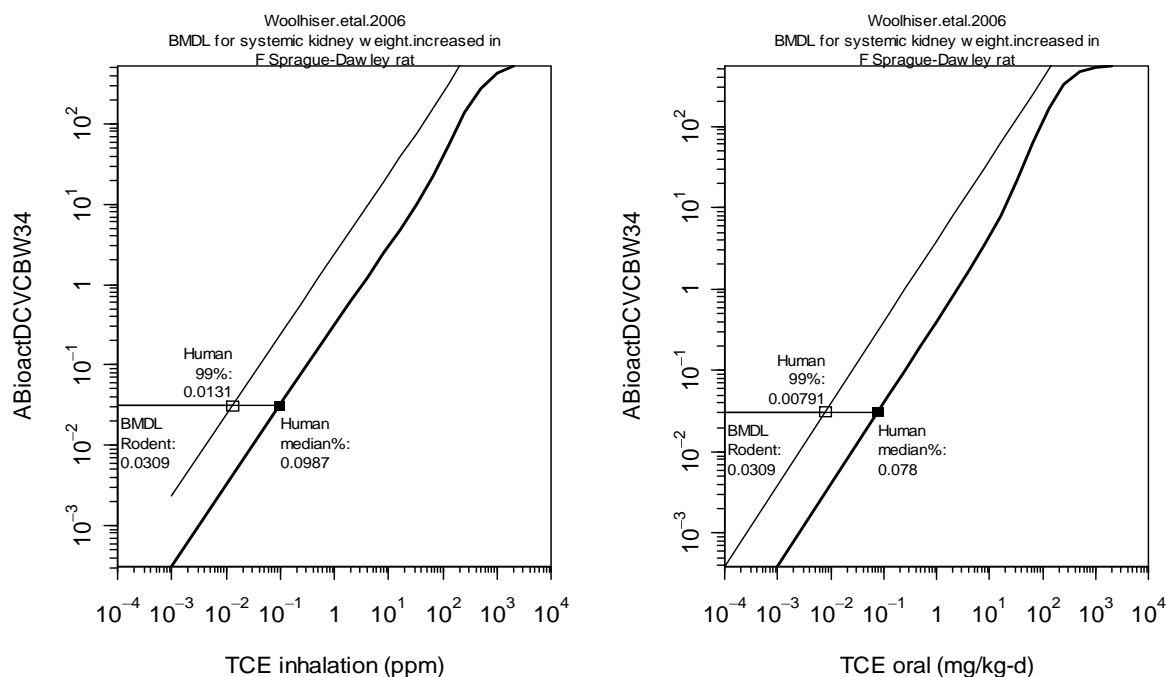


Figure F-13. Derivation of HEC₉₉ and HED₉₉ corresponding to the rodent idPOD from Woolhiser et al. (2006) for increased kidney weight in rats.

F.6.3. Keil et al. (2009)—LOAEL for Decreased Thymus Weight in Mice

The critical endpoint here is decreased thymus weight in female B6C3F₁ mice (Keil et al., 2009).

F.6.3.1. Dosimetry

Mice were exposed to 1,400 and 14,000 ppb of TCE in drinking water, with an average dose estimated by EPA to be 0.35 and 3.5 mg/kg/day, for 30 weeks, based on the average of subchronic and chronic values for generic body weight and water consumption rates for female B6C3F1 mice (U.S. EPA, 1988). The dose-response relationships were sufficiently supralinear that BMD modeling failed to produce an adequate fit. The primary dose-metric was selected to be the average amount of TCE metabolized/kg^{3/4}/day. The lower dose group was the LOAEL, and the median estimate from the PBPK model at that exposure level was 0.139 mg TCE metabolized/kg^{3/4}/day, which is used as the rodent idPOD.

F.6.3.2. Derivation of HEC₉₉ and HED₉₉

The HEC₉₉ and HED₉₉ are the lower 99th percentiles for the continuous HEC and continuous human ingestion dose that lead to a human internal dose equal to the rodent idPOD. The derivation of the HEC₉₉ of 0.0332 ppm and HED₉₉ of 0.0482 mg/kg/day for the 99th percentile for uncertainty and variability are shown in Figure F-14. These values are used as this critical effect's POD to which additional UFs are applied.

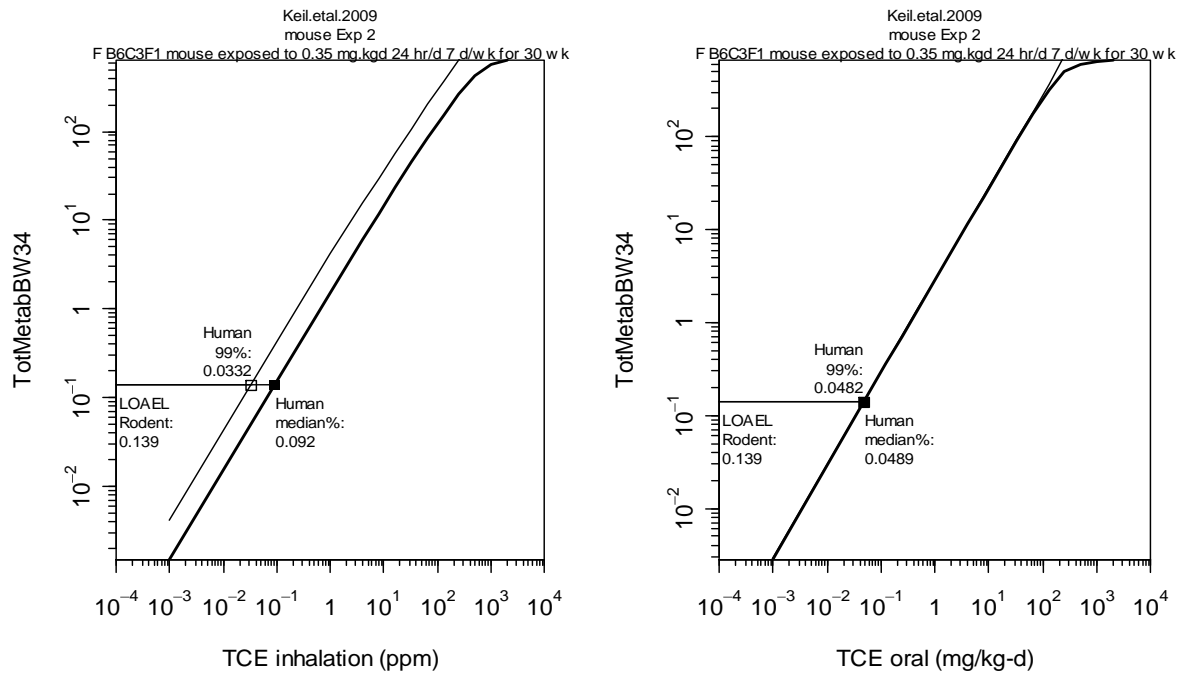


Figure F-14. Derivation of HEC₉₉ and HED₉₉ corresponding to the rodent idPOD from Keil et al. (2009) for decreased thymus weight in mice.

F.6.4. Johnson et al. (2003)—BMD Modeling of Fetal Heart Malformations in Rats

The critical endpoint here is increased fetal heart malformations in female Sprague-Dawley rats (Johnson et al., 2003).

F.6.4.1. Dosimetry and BMD Modeling

Rats were exposed to 2.5, 250, 1.5, or 1,100 ppm TCE in drinking water for 22 days (GDs 1–22). The primary dose-metric was selected to be average amount of TCE metabolized by oxidation/kg^{3/4}/day, with median estimates from the PBPK model for this study of 0.00031, 0.033, 0.15, and 88.

As discussed previously in Section F.4.2.1, from results of nested log-logistic modeling of these data, with the highest dose group dropped, the idPOD of 0.0142 mg TCE metabolized by oxidation/kg^{3/4}/day was a BMDL for a BMR of 1% increased in incidence in pups. A 1% extra risk of a pup having a heart malformation was used as the BMR because of the severity of the effect; some of the types of malformations observed could have been fatal.

F.6.4.2. Derivation of HEC₉₉ and HED₉₉

The HEC₉₉ and HED₉₉ are the lower 99th percentiles for the continuous HEC and continuous human ingestion dose that lead to a human internal dose equal to the rodent idPOD. The derivation of the HEC₉₉ of 0.00365 ppm and HED₉₉ of 0.00515 mg/kg/day for the 99th percentile for uncertainty and variability are shown in Figure F-15. These values are used as this critical effect's POD to which additional UFs are applied.

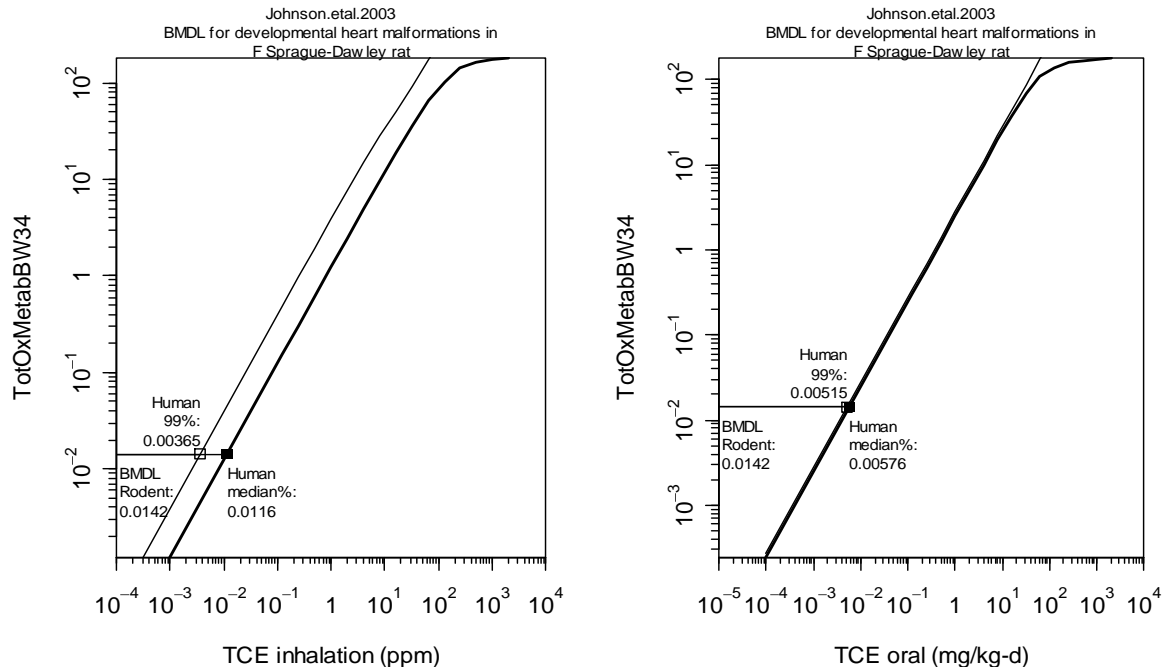


Figure F-15. Derivation of HEC₉₉ and HED₉₉ corresponding to the rodent idPOD from Johnson et al. (2003) for increased fetal cardiac malformations in female Sprague-Dawley rats using the total oxidative metabolism dose-metric.

F.6.5. Peden-Adams et al. (2006)—LOAEL for Decreased PFC Response and Increased Delayed-Type Hypersensitivity in Mice

The critical endpoints here are decreased PFC response and increased delayed-type hypersensitivity in mice exposed pre- and postnatally (Peden-Adams et al., 2006).

Mice were exposed to 1,400 and 14,000 ppb in drinking water, with an average dose in the dams estimated by the authors to be 0.37 and 3.7 mg/kg/day, from GD 0 to postnatal ages of 3 or 8 weeks. The dose-response relationships were sufficiently supralinear that BMD modeling failed to produce an adequate fit. In addition, because of the lack of an appropriate PBPK model and parameters to estimate internal doses given the complex exposure pattern (placental and lactational transfer, and pup ingestion postweaning), no internal dose estimates were made. Therefore, the LOAEL of 0.37 mg/kg/day on the basis of applied dose was used as the critical effect's POD to which additional UFs are applied.